Talanta 97 (2012) 400–405

Contents lists available at SciVerse ScienceDirect

Talanta

journal homepage: www.elsevier.com/locate/talanta

Combined corona discharge and UV photoionization source for ion mobility spectrometry

Hamed Bahrami, Mahmoud Tabrizchi *

Department of Chemistry, Isfahan University of Technology, Isfahan 84156-83111, Iran

ARTICLE INFO

Article history:
Received 29 February 2012
Received in revised form
22 April 2012
Accepted 24 April 2012
Available online 3 May 2012

Keywords:
Ion mobility
UV photoionization
Corona discharge
Ionization source

ABSTRACT

An ion mobility spectrometer is described which is equipped with two non-radioactive ion sources, namely an atmospheric pressure photoionization and a corona discharge ionization source. The two sources cannot only run individually but are additionally capable of operating simultaneously. For photoionization, a UV lamp was mounted parallel to the axis of the ion mobility cell. The corona discharge electrode was mounted perpendicular to the UV radiation. The total ion current from the photoionization source was verified as a function of lamp current, sample flow rate, and drift field. Simultaneous operation of the two ionization sources was investigated by recording ion mobility spectra of selected samples. The design allows one to observe peaks from either the corona discharge or photoionization individually or simultaneously. This makes it possible to accurately compare peaks in the ion mobility spectra from each individual source. Finally, the instrument's capability for discriminating two peaks appearing in approximately identical drift times using each individual ionization source is demonstrated.

1. Introduction

Ion mobility spectrometry (IMS) emerged as an analytical technique in the early 1970s [1]. In IMS, sample vapors are converted into ions at atmospheric pressure. The ions are then identified by measuring their mobility in an electric field. In practice, the electric field conducts ions created by the ionization source into the reaction region. Pulses of ions are subsequently injected into the drift region by a shutter grid, where they are separated under the action of an external electric field and collision with a counter-moving drift gas. Low ppb range detection limits and fast response times of just a few seconds make this technique extremely useful. Rapid determination of different compounds by hand-held IMS devices has nowadays become a routine technique. IMS is widely used for detecting explosives [2,3], chemical warfare agents [4], and illicit drugs [5]. In addition, IMS is a well-established technique for the analysis of materials under ambient conditions in the open air [6].

The ionization source plays a key role in the IMS instrument. Conventional IMS instruments use radioactive ^{63}Ni which is favored due to its simplicity, stability, convenience, and no need for an external power supply. However, this source is disadvantageous for its limited linear range and the regulatory requirements associated with radioactive materials. In recent decades, many ionization sources have been investigated including X-ray ionization [7], surface ionization [8,9], laser ionization [10,11], electrospray ionization [12,13], atmospheric pressure photoionization (APPI) [14,15], continuous or pulsed corona discharge ionization [16–18], corona spray ionization [19], thermal ionization [20], and low-temperature plasma [21].

Corona discharge (CD) ionization can be used for ionizing a broad range of chemical compounds [22–24]. The dominant reactant ions produced in the positive corona discharge in air or in nitrogen include $(H_2O)_nH^+$ [25]. Hence, compounds with high proton affinity are easily ionized via proton transfer in the corona discharge but with the disadvantage that the reactant ion peak (RIP) may interfere with the analyte peak. This is the case with benzene whose peak overlays on the RIP. Another drawback associated with CD is the occasional crowding of the spectra due to different protonation schemes or fragmentation. UV photoionization may be regarded as a complement to the CD-IMS since it produces no background peaks. Additionally, the use of UV photoionization source broadens the range of classes of compounds (such as nonpolar molecules not easily ionized by CD) that can be analyzed by IMS instruments. Terpenes [26] and alcohols [27] are examples of compounds that are successfully analyzed by UV-IMS. UV photoionization is sometimes more selective than CD. Compounds such as acetone in urine, which is a biomarker for cow and human diseases, can be readily analyzed by UV-IMS despite the presence of ammonia in urine.

* Corresponding author. Tel.: +98 311 3913272; fax: +98 311 3912350.
E-mail address: m-tabriz@cc.iut.ac.ir (M. Tabrizchi).

0039-9140/$ - see front matter © 2012 Elsevier B.V. All rights reserved.
http://dx.doi.org/10.1016/j.talanta.2012.04.052

This is because ammonia is not ionized by direct photoionization [28]. Unlike the case of UV source, acetone is not ionized by CD in the presence of ammonia because of its lower proton affinity.

The aim of this paper is to design an IMS apparatus which is capable of working with both CD and UV ionization sources. These sources have already been compared in terms of their performance using IMS instruments with either CD or UV and reported elsewhere [29–31]. The responses of two similar made spectrometers are not necessarily identical. Hence, comparison of ion mobility spectra using separate instruments cannot be reliable. A true comparison requires the two ion sources to be investigated in one single instrument. Recently, Adamov et al., designed and built an IMS instrument that allowed rapid switching of different atmospheric pressure ionization modes, namely ESI, CD, UV, and radioactive ^{63}Ni [32]. This multi-ion source platform allows for fast and easy switching between four different atmospheric pressure ionization methods and, thus, eliminates any possible errors caused by differences among instruments equipped with different ionization sources. Nonetheless, Adamov et al. did not report the simultaneous operation of two ionization sources. In this work, we describe the simultaneous use of CD and UV ionization sources in one single IMS instrument and demonstrate the advantage of simultaneous running of two ion sources.

2. Experimental

A detailed description of the design of the reaction region and drift tube may be found in our previous works [16,33]. The IMS used in the present study was manufactured at Isfahan University of Technology (Fig. 1) and consisted of both an ionization and a drift region, housed in a thermostatic oven with temperatures ranging from room temperature to 500 K within ± 2 K. The ionization region consisted of four aluminum rings with 0.95 cm thickness, 20 mm ID and 55 mm OD. The drift tube consisted of 11 similar aluminum rings of 36 mm ID. An additional similar ring hosting a shutter grid was placed between the two regions in order to separate the ionization region from the drift region. Thin Teflon insulators were inserted between the rings. Each ring was connected to the adjacent one via a 5 MΩ resistor to create a potential gradient. A voltage of 7 kV was applied across the entire cell to create a drift field of 437 V cm^{-1}. The shutter grid was operated by applying a 100 μs pulse of 110 V amplitude. This allowed ions to pass through during the short period of removed voltage. A faraday cup detector was located at the end of the drift tube and encapsulated in a stainless steel chamber. The collected signal was amplified with a gain of 10^9 V/A and fed to a computer via a digital oscilloscope (ADC212 Picotech, UK).

A home-made nebulizer capable of working up to 520 K was used for the IMS experiments. Nitrogen was used for both the nebulizer and the drift gas at flow rates of 200 mL min^{-1} and 800 mL min^{-1}, respectively. The injection port and the drift tube temperatures were 493 and 473 K, respectively.

A vacuum–UV Krypton lamp powered by a 1.2 kV DC power supply was used as the UV photoionization source to emit UV light at 10 and 10.6 eV. The lamp was mounted in a cylindrical support made of PTFE Teflon. A detailed description of the photoionization source employed is given in our previous work [15]. The corona electrode, mounted on the first ring of the ionization region, was a sharp needle made of stainless steel with a Teflon isolating cover.

2.1. Sample preparation

Analytical grade toluene and anisole was used as the sample and the dopant while methanol was used as the solvent, both purchased from Merck. The chemicals (acridine, nicotine and caffeine) were obtained from Merck and used without further purification. Standard solutions were made by solving the chemicals in methanol. Working standard solutions were prepared by consecutive dilution of the standard solutions. 2 μL of the working solution was loaded into the injection port and the solvent was allowed to evaporate. Toluene in vapor form was used as the dopant or the sample. A syringe pump (New Era Pump System Inc. USA) was used to inject head space vapor of toluene into the ionization region at a flow rate of 300 μL min^{-1}. The preferred concentration of toluene was obtained via pump speed adjustments.

The drift and carrier gas supply used in this work was pure nitrogen. In order to remove water vapor and other contaminants, the gas was filtered by passing through a 13 × molecular sieve (Fluka) trap before entering into the IMS tube.

3. The design

Generally speaking, either of two designs is possible for the UV-IMS. In the first, the lamp may be mounted perpendicular to the direction of the IMS cell axis (side-mount) [34]. Alternatively, it can be installed on-axis (head-mount) [14,35]. The latter design yielded better sensitivity and limits of detection [14,15]. In this geometry, the UV light propagates deeply into the ionization region, providing a longer interaction zone between the UV light and the molecules; hence, a better ionization yield. Moreover, the UV light does not interfere with the operation of the drift tube since a major portion of the light is absorbed within a short distance from the window leaving only a small amount to reach the drift tube. The lamp was, therefore, mounted parallel and on-center to the axis of the drift tube. The corona needle was installed perpendicular to the UV radiation in order to minimize

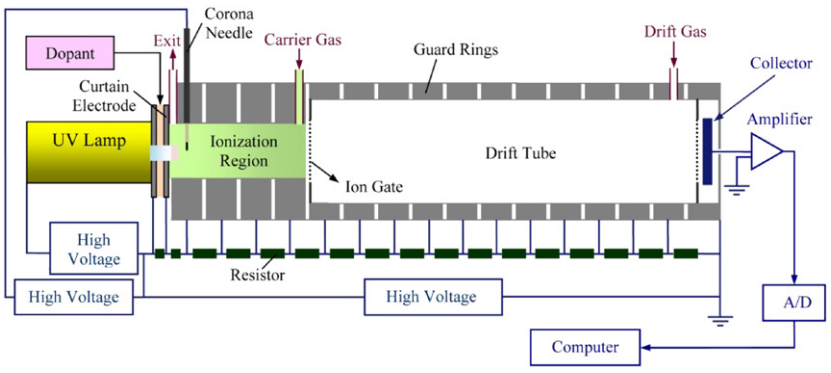

Fig. 1. Schematic view of the ion mobility spectrometer.

its interference with the UV source. The schematic diagram of the new design is shown in Fig. 1.

Ionization efficiency in UV ionization is commonly enhanced by using a dopant, as sample molecules are ionized via charge transfer with the dopant photoions. A curtain region was designed in front of the lamp for two reasons: first, to have a shield gas in front of the lamp in order to prevent deposition of the sample on the window; and second, to divide the ionization zone into two distinct regions: the dopant and the sample regions. This was achieved by mounting a stainless steel disk with a 3 mm hole in the center, called a curtain electrode, at a distance of 5 mm from the lamp head. A flow of dry nitrogen (about 40 μL min^{-1}) was introduced between the lamp and the disk, which was then exited through the hole in the curtain electrode. A voltage of 600 V was applied through the resistor chain between the lamp head and the curtain electrode in order to pull the photoions generated in front of the lamp into the dopant region towards the solvent. The dopant was introduced in the vicinity of the lamp and the vaporized sample or solvent (if present) was introduced into the sample region. The curtain electrode prevented the solvent from entering the dopant region where the dopant was directly photoionized. This prevented the negative effect of the solvent on the photoionization yield so that the dopant would be effectively ionized. The performance and effectiveness of the curtain electrode is given in our recent work [15].

4. Results and discussion

4.1. Total ion current

In order to investigate the behavior of the UV lamp as an ionization source in ion mobility spectrometry, the total ion current produced by the UV source was initially measured as a function of toluene concentration, lamp current, and drift field. In these experiments, the shutter grid was open and toluene, as a test sample, was injected into the ionization region.

Fig. 2(a) shows the total ion current on the detector as a function of toluene flow rate for different lamp intensities at a fixed drift field of 437 V cm^{-1}. For all lamp intensities, an increase was observed in the total ion current by increasing toluene flow rate. The current reached an upper limit of about 4.6 nA at a toluene flow rate of 950 μL min^{-1} and a lamp current of 1.5 mA. TIC was also measured as a function of lamp current at different drift fields. The results shown in Fig. 2(b) indicate that the current increased by increasing the lamp current.

We have previously shown in the case of corona discharge that increasing drift field leads to an increase in TIC [16]. To compare, the total photoion current was also measured as a function of drift field for different lamp currents ranging from 0.5 to 1.5 mA, as shown in Fig. 3. For comparison, the TIC values obtained from corona discharge under identical conditions are plotted versus drift field. It clearly fits well in a quadratic function. The photoion current also grows quadratically but, unlike the case of corona discharge, it deviates and reaches an upper limit. This reveals that the initial ion current for the case of UV source is less than that of the corona discharge, so that applying a higher electric field to increase collection efficiency will not lead to a higher ion current.

4.2. Ion mobility spectra

4.2.1. Operating individual ion sources

Fig. 4 illustrates the background ion mobility spectra using both corona discharge and photoionization sources individually.

For the CD ionization source, three reactant ion peaks corresponding to $(H_2O)_nH^+$, NO^+ and NH_4^+, were observed in agreement with previous ion mobility studies. When the CD was off and the UV lamp was running, a flat zero baseline was observed. Since the ionization potential of nitrogen (15.58 eV) is considerably higher than the energy of the 10.0 eV Kr lamp, no ionization occurs and, hence, no peaks are observed.

Positive ion mobility spectra of toluene and anisole were obtained using CD and UV ionization sources individually. As shown in Fig. 5(a), in the case of toluene, the CD spectrum consists of two

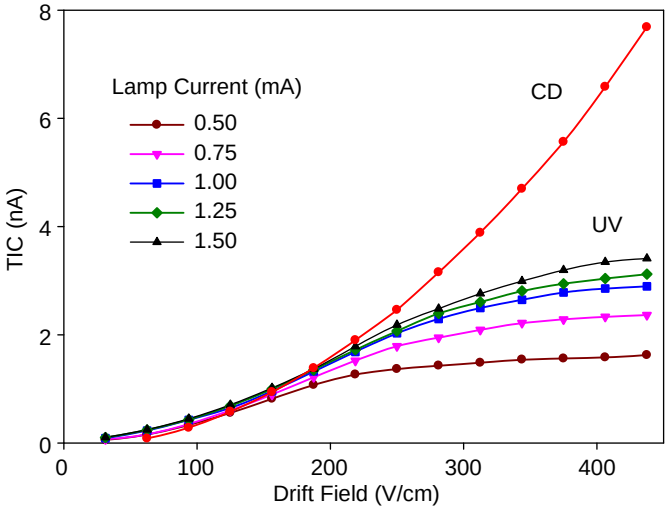

Fig. 3. Total UV–ion current as a function of drift field for different lamp intensities compared with that of corona discharge under identical conditions.

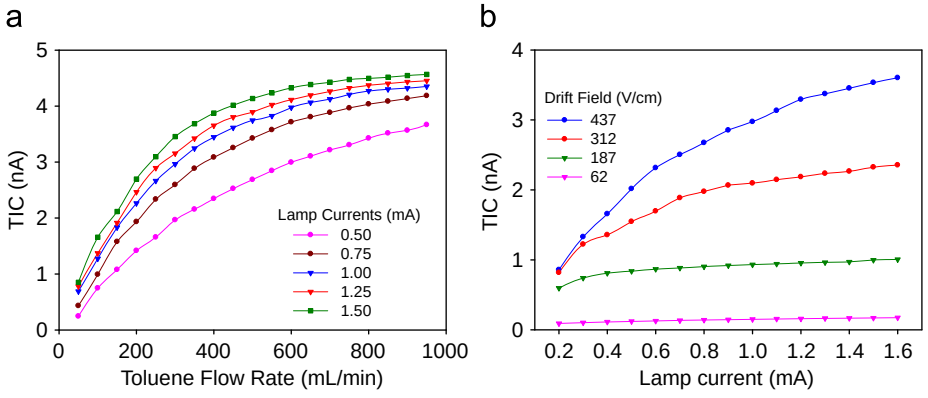

Fig. 2. (a) Total ion current as a function of toluene flow rate for different lamp intensities and (b) as a function of UV lamp current at different drift fields.

main product ion peaks while the UV spectrum provides one single product ion peak.

In the case of toluene, it is clear that different product ion peaks are obtained with CD and UV. The peak in the UV spectrum is the M^+ product ion since krypton lamp (10 eV) directly photoionizes toluene. This peak is repeated in the CD spectrum. In addition to the M^+ peak, a second peak is observed in the CD spectrum, which may be assigned to $[MH]^+$. This example clearly demonstrates that the two ionization mechanisms, namely proton transfer and charge transfer, are active in the corona discharge.

Unlike toluene, the ion mobility spectrum of anisole in CD and UV sources contains only one main peak. At first glance, the two peaks seem similar. However, close investigation shows that they are slightly different. In order to prove that the two seemingly similar peaks are different, the two ionization sources must be run simultaneously.

4.2.2. Combined ionization sources

The importance of combining two ion sources is demonstrated below. The ion mobility spectrum of anisole was recorded by simultaneously running two ion sources. As shown in Fig. 6, two peaks are observed very close to each other. This proves that, despite their proximity, the peaks in Fig. 5(b) are different indeed. Like toluene, the two peaks may be attributed to M^+ and MH^+.

Fig. 7 shows the ion mobility spectra of acridine under four different sets of conditions, CD only, UV only, UV+dopant, and CD+UV+dopant. While UV and CD ionization sources are run individually, only one main product ion peak differing by 0.15 ms is observed in each spectrum. Again, these peaks can be attributed to M^+ and MH^+ for UV and CD spectra, respectively. In the case of UV only, when toluene is introduced as a dopant in the ionization region, the M^+ peak grows considerably and the MH^+ peak appears as well. In fact, the dopant facilitates ion formation by converting photons to primary ions. Secondary ions are then formed via a charge transfer reaction with the ionized dopant. A second ionization mechanism is proton transfer from the ionized dopant to the analyte, which also gives rise to the MH^+ peak. The dopant opens another channel of ionization. The relative intensities, in this case, reveal that the charge transfer is the dominant mechanism. Simultaneous running of the two ion sources, in the presence of toluene as the dopant, yielded two peaks, similar to the dopant-assisted UV spectrum. However, the intensities of the two peaks swapped with respect to the UV-dopant spectrum. This is because of increasing protonated reactant ions including H_3O^+ and toluene-H^+ when CD is switched on.

4.2.3. Calibration curves

The calibration curve for acridine, as a test compound, was obtained under optimized conditions for both CD and UV ionization sources, as shown in Fig. 8. The area under all corresponding peaks for the sample was considered as the response. The limits of detection for acridine, defined as the amount giving peak height

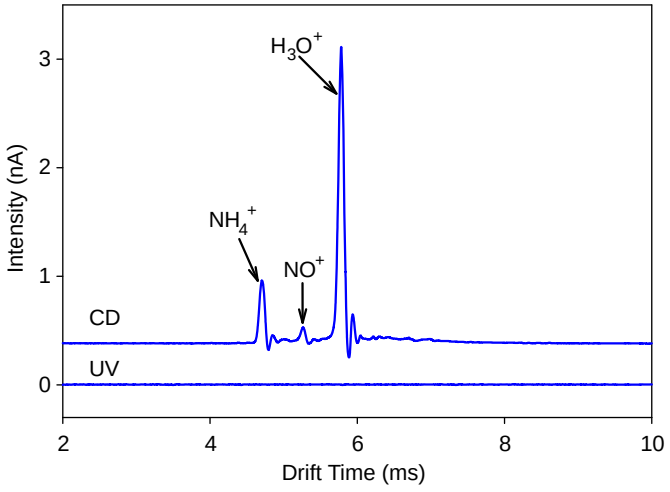

Fig. 4. Comparison of positive ion mobility spectra resulting from corona discharge and UV lamp.

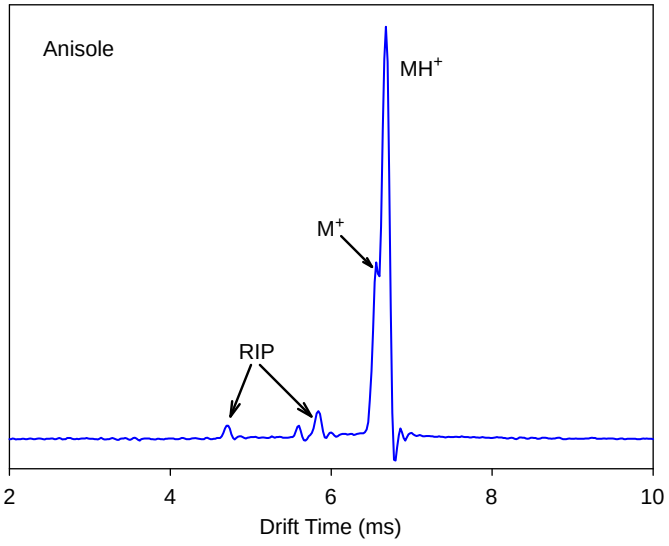

Fig. 6. Ion mobility spectrum of anisole with simultaneous CD and UV ionization sources.

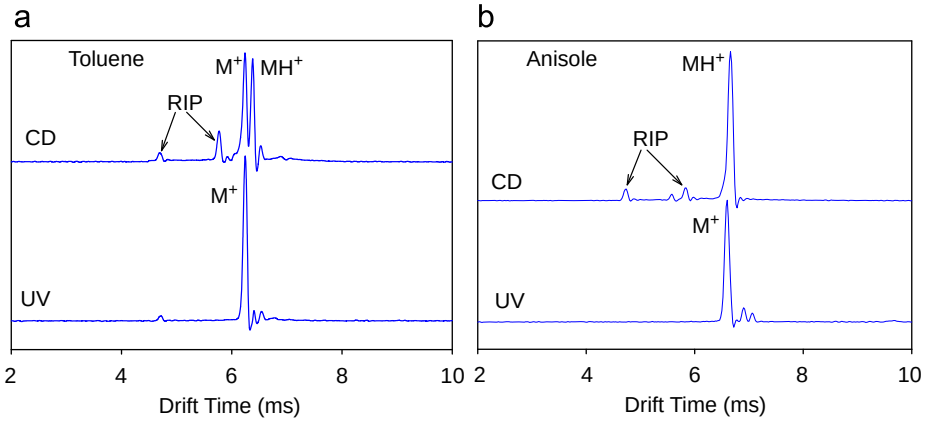

Fig. 5. Ion mobility spectra of toluene and anisole with individual UV and CD ionization sources.

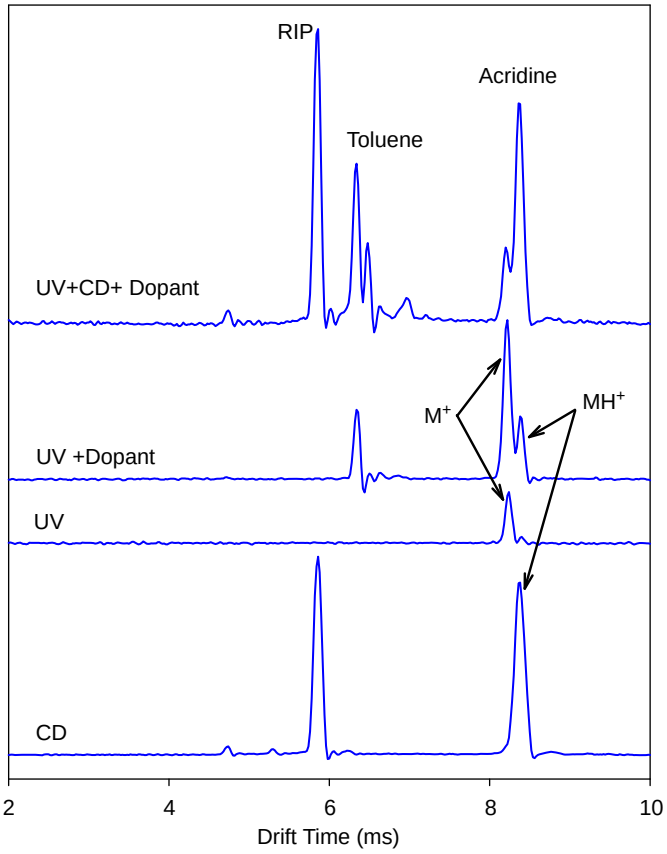

Fig. 7. Ion mobility spectrum of acridine with separate and simultaneous ion sources.

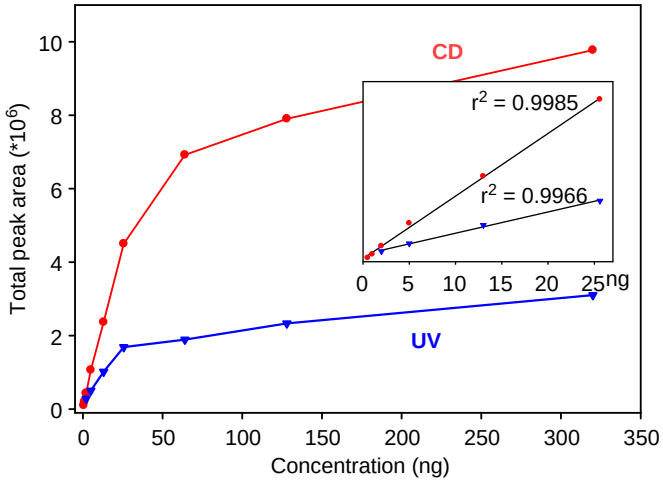

Fig. 8. Calibration curves for acridine for CD and UV ionization sources.

three times the noise level, were obtained to be 0.11 and 0.30 ng for CD and UV, respectively.

4.2.4. *The inverse mode*

We recently introduced a novel method to increase the resolution of IMS [36]. This method is based on applying an inverse pulse to the shutter grid, i.e., where an empty space (i.e., a gap rather than an ion packet) travels through a bath of ions. The space charge of ions tends to narrow the gap and a better resolution can thus be achieved. Using this technique, two close peaks that were not resolved via normal IMS were well resolved

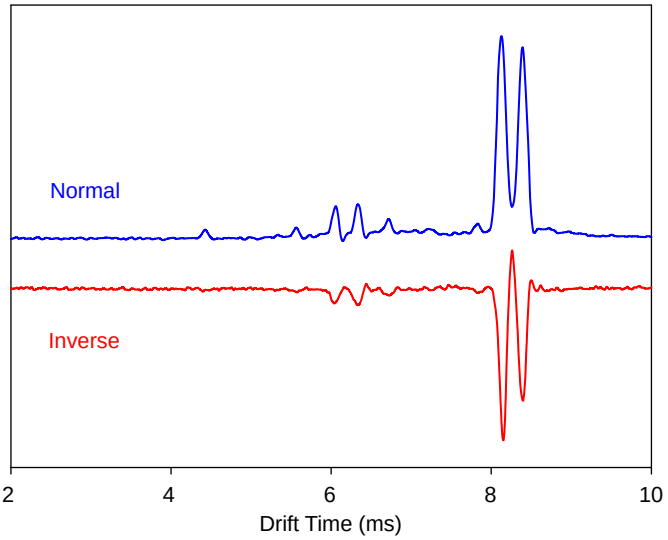

Fig. 9. Ion mobility spectrum of caffeine in normal and inverse modes, using the UV-ionization source. The overlapping peaks are well resolved using the inverse mode.

to the baseline. The reason for the increased resolution is the absence of space charge in the gap. For two neighboring gaps, a layer of ions is trapped between the two gaps. These ions are under a sandwich force from the ion clouds on both sides. As a result, the trapped swarm of ions gets narrower; thus, increasing the baseline resolution for the two neighboring dips.

This technique was examined for ion mobility spectrometer with the UV-photoionization source. An experiment was performed to show the ability of the inverse mode of operation in resolving two adjacent peaks. Caffeine shows a double peak in its ion mobility spectrum in the presence of an appropriate dopant. Fig. 9 compares its spectra for the cases of normal and inverse operation using the UV ionization source. A normal spectrum was recorded under optimum conditions with the best resolution. The inversed spectrum was recorded under conditions that resulted in almost the same intensity as that in the normal mode. Obviously, unlike in the normal mode, the overlapping peaks are resolved to the baseline in the inverse mode.

5. Conclusions

In this work, an IMS instrument with two simultaneous ion sources was developed. Corona discharge is a powerful ionization source that ionizes species with high proton affinity. Furthermore, UV photoionization is a primary ionization source which ionizes species with low ionization energy. The combination of the two sources is found to compensate for the limitations of each single source. The design enables fast and easy switching between the two ionization methods without the need to remove one. This allows a wide range of analytes to be measured while it also eliminates the errors in reduced mobilities caused by switching the instrument off and on.

Another advantage of the design is that the two ionization sources can operate simultaneously. Such a combination provides the possibility for accurately comparing the peaks obtained by either UV or CD ionization. This is especially important in assigning IMS peaks to their origins and in studying ion molecule reactions. Finally, the experiments showed that the inverse technique yields improved IMS resolution when the instrument is equipped with a UV ionization source.

Acknowledgments

The authors would like to acknowledge the financial support of the Center of Excellence for Sensor and Green Chemistry. Also, the authors would like to appreciate Dr. H. Farrokhpour for valuable discussions and V. Ilbeigy for her invaluable assistance. Prof. M Blade of the University of British Columbia is also acknowledged for his support in providing the UV source.

References

[1] M.J. Cohen, F.W. Karasek, J. Chromatogr. Sci. 8 (1970) 330–337.
[2] A.B. Kanu, H.H. Hill Jr., Talanta 73 (2007) 692–699.
[3] R.G. Ewing, D.A. Atkinson, G.A. Eiceman, G.J. Ewing, Talanta 54 (2001) 515–529.
[4] A.B. Kanu, P.E. Haigh, H.H. Hill, Anal. Chim. Acta 553 (2005) 148–159.
[5] J.K. Lokhnauth, N.H. Snow, J. Sep. Sci. 28 (2005) 612–618.
[6] R.B. Cody, J.A. Laramée, H.D. Durst, Anal. Chem. 77 (2005) 2297–2302.
[7] V.S. Pershenkov, A.D. Tremasov, V.V. Belyakov, A.U. Razvalyaev, V.S. Mochkin, Microelectron. Reliab. 46 (2006) 641–644.
[8] C. Wu, H.H. Hill, U.K. Rasulev, E.G. Nazarov, Anal. Chem. 71 (1999) 273–278.
[9] H.-Y. Guo, X.-L. He, X.-G. Gao, J. Jia, J.-P. Li, Anal. Chim. Acta 587 (2007) 137–141.
[10] H.-G. Löhmannsröben, T. Beitz, R. Laudien, R. Schultze, Proc. Soc. Photo-Opt. Intrum. Eng. 5547 (2004) 16–24.
[11] G.E. Kotkovskii, I.L. Martynov, V.V. Novikova, A.A. Chistyakov, Instrum. Exp. Tech. 52 (2009) 253–259.
[12] T. Khayamian, M.T. Jafari, Anal. Chem. 79 (2007) 3199–3205.
[13] C.A. Krueger, C.K. Hilton, M. Osgood, J. Wu, C. Wu, Int. J. Ion Mobil. Spec. 12 (2009) 33–37.
[14] C.S. Leasure, M.E. Fleischer, G.K. Anderson, G.A. Eiceman, Anal. Chem. 58 (1986) 2142–2147.
[15] M. Tabrizchi, H. Bahrami, Anal. Chem. 83 (2011) 9017–9023.
[16] M. Tabrizchi, T. Khayamian, N. Taj, Rev. Sci. Instrum. 71 (2000) 2321–2328.
[17] M. Tabrizchi, A. Abedi, Int. J. Mass Spectrom. 218 (2002) 75–85.
[18] J. Xu, W.B. Whitten, J.M. Ramsey, Anal. Chem. 75 (2003) 4206–4210.
[19] C.B. Shumate, H.H. Hill, Anal. Chem. 61 (1989) 601–606.
[20] M. Tabrizchi, Anal. Chem. 75 (2003) 3101–3106.
[21] M.T. Jafari, Anal. Chem. 83 (2011) 797–803.
[22] H.-Y. Han, G.-D. Huang, S.-P. Jin, P.-C. Zheng, G.-H. Xu, J.-Q. Li, H.-M. Wang, Y.-N. Chu, J. Environ. Sci. 19 (2007) 751–755.
[23] H. Borsdorf, H. Schelhorn, J. Flachowsky, H.-R. Döring, J. Stach, Anal. Chim. Acta 403 (2000) 235–242.
[24] M. Tabrizchi, V. Ilbeigi, J. Hazard. Mater. 176 (2010) 692–696.
[25] M. Pavlik, J.D. Skalny, Rapid Commun. Mass Spectrom. 11 (1997) 1757–1766.
[26] W. Vautz, S. Sielemann, J.I. Baumbach, Anal. Chim. Acta 513 (2004) 393–399.
[27] St. Sielemann, J.I. Baumbach, H. Schmidt, P. Pilzecker, Anal. Chim. Acta 431 (2001) 293–301.
[28] R. Garrido-Delgadoa, L. Arcea, C.C. Pérez-Marínb, M. Valcárcela, Talanta 78 (2009) 863–868.
[29] H. Borsdorf, M. Rudolph, Int. J. Mass Spectrom. 208 (2001) 67–72.
[30] H. Borsdorf, E.G. Nazarov, G.A. Eiceman, Int. J. Mass Spectrom. 232 (2004) 117–126.
[31] H. Borsdorf, K. Neitsch, G.A. Eiceman, J.A. Stone, Talanta 78 (2009) 1464–1475.
[32] A. Adamov, T. Mauriala, V. Teplov, J. Laakia, C.S. Pedersen, T. Kotiaho, A.A. Sysoev, Int. J. Mass Spectrom. 298 (2010) 24–29.
[33] M. Tabrizchi, Iranian Patent no. 42767, 2007.
[34] M.A. Baim, R.L. Eatherton, H.H. Hill, Anal. Chem. 55 (1983) 1761–1766.
[35] C. Chen, C. Dong, Y. Du, S. Cheng, F. Han, L. Li, W. Wang, K. Hou, H. Li, Anal. Chem. 82 (2010) 4151–4157.
[36] M. Tabrizchi, E. Jazan, Anal. Chem. 82 (2010) 746–750.